HHS Public Access

Author manuscript

Neuroendocrinology. Author manuscript; available in PMC 2015 November 07.

Published in final edited form as:

Neuroendocrinology. 2014 ; 100(0): 228–239. doi:10.1159/000369467.

GPER1 stimulation alters posttranslational modification of RGSz1 and induces desensitization of 5-HT$_{1A}$ receptor signaling in the rat hypothalamus

Carrie E McAllister, PhD[1], **Zhen Mi, BS**[1], **Minae Mure, PhD**[2], **Qian Li, PhD**[3], and **Nancy A Muma, PhD**[1,*]

[1]Department of Pharmacology and Toxicology, University of Kansas

[2]Department of Chemistry, University of Kansas

[3]Division of Gastroenterology and Hepatology, Johns Hopkins University School of Medicine

Abstract

Hyperactivity of the hypothalamic-pituitary-adrenal axis is a consistent biological characteristic of depression and response normalization coincides with clinical responsiveness to antidepressant medications. Desensitization of serotonin 1A receptor (5-HT$_{1A}$R) signaling in the hypothalamic paraventricular nucleus (PVN) follows selective serotonin reuptake inhibitor (SSRI) antidepressant treatment and contributes to the antidepressant response. Estradiol alone produces a partial desensitization of 5-HT$_{1A}$R signaling, and synergizes with SSRIs to result in a complete and more rapid desensitization than with SSRIs alone as measured by a decrease in the oxytocin and adrenocorticotrophic hormone(ACTH) responses to 5-HT$_{1A}$R stimulation. G protein-coupled estrogen receptor1 (GPER1) is necessary for estradiol-induced desensitization of 5-HT$_{1A}$R signaling, although the underlying mechanisms are still unclear. We now find that stimulation of GPER1 with the selective agonist G-1 and non-selective stimulation of estrogen receptors dramatically alter isoform expression of a key component of the 5-HT$_{1A}$R signaling pathway, RGSz1, a GTPase activating protein selective for Gαz, the Gα subunit necessary for 5-HT$_{1A}$R-mediated hormone release. RGSz1 isoforms are differentially glycosylated, SUMOylated, and phosphorylated, and differentially distributed in subcellular organelles. High molecular weight RGSz1 is SUMOylated and glycosylated, localized to the detergent-resistant microdomain (DRM) of the cell membrane, and increased by estradiol and G-1 treatment. Because activated Gαz also localizes to the DRM, increased DRM-localized RGSz1 by estradiol and G-1could reduce Gαz activity, functionally uncoupling 5-HT$_{1A}$R signaling. Peripheral G-1 treatment produced partial reduction in oxytocin and ACTH responses to 5-HT$_{1A}$R-stimulation similar to direct injections into the PVN. Together, these results identify GPER1 and RGSz1 as novel targets for the treatment of depression.

*Corresponding Author: Nancy A. Muma, Malott Hall Rm 5064, 1251 Wescoe Hall Dr., Lawrence, KS 66045-7572, nmuma@ku.edu, Telephone: +1 785 864 4002, Fax: +1 785 864 5219.

Conflict of Interest

The authors declare no conflict of interest.

Keywords

5-HT_{1A} receptor; GPER1; estradiol; RGSz1; G-1; SUMOylation; phosphorylation; glycosylation; HPA

Introduction

The most consistent biomarker in depressed patients is increased hypothalamic-pituitary-adrenal (HPA) axis activity, such as high levels of plasma corticotropin releasing hormone (CRH), adrenocorticotrophic hormone (ACTH), and cortisol [1; 2], and successful antidepressant treatment is frequently correlated with normalization of HPA axis activity [3]. Serotonin is a major mediator of the HPA axis [4]; recent studies have shown that depression-like behavior in rodents is modulated by serotonin receptors, in particular the serotonin 1A receptor (5-HT_{1A}R) [5; 6].

Selective stimulation of 5-HT_{1A}R with (+)8-OH-DPAT produces an increase in the plasma levels of oxytocin (OT), ACTH, and corticosterone, which can be prevented by treatment with the 5-HT_{1A}R antagonist WAY 100 635 in the paraventricular nucleus of the hypothalamus (PVN)[7; 8]. Chronic treatment with SSRIs produces desensitization of 5-HT_{1A}R signaling in the PVN, as measured by a reduction in the OT and ACTH response to 5-HT_{1A}R stimulation [9; 10; 11]. It takes 3–12 weeks to achieve clinical efficacy with SSRIs [12; 13]. Since this therapeutic delay is thought to be partly due to the time it takes for desensitization of 5-HT_{1A}R signaling in the PVN and contribute to normalization of the HPA axis, treatment that reduces the time to achieve desensitization could have tremendous therapeutic benefits [9; 14; 15; 16].

Neuroendocrine challenge tests that detect peripheral changes in hormone responses to 5-HT_{1A}R agonists can be used to measure desensitization of 5-HT_{1A}R signaling in the PVN [8; 17]. We found that two-day estradiol treatment accelerates SSRI-induced 5-HT_{1A}R desensitization [18]; however, the mechanism underlying this effect is still unclear. Minimal estrogen receptor (ER) α is expressed in the PVN, though it is abundant in the peri-PVN region [19]. ERβ is abundantly expressed in the PVN and importantly in OT expressing neurons and a subset of CRH expressing neurons [20; 21] but does not contribute to the desensitization of 5-HT_{1A}R signaling in the PVN, as selective stimulation of ERβ does not produce the desensitization response and knocking down ERβ in the PVN does not prevent the desensitization response [22].

Several G protein-coupled ERs have been reported. A Gαq-coupled receptor is expressed in the arcuate nucleus of the hypothalamus, CA1 region of the hippocampus and primary cortical cells in culture but not in the PVN [23]. G protein-coupled estrogen receptor 1 (GPER1, also known as GPR30) distribution in the brain is distinct from ERα or ERβ [24], and colocalizes with 5-HT_{1A}R, OT, and CRH in the PVN [24; 25; 26; 27], demonstrating that GPER1 is positioned to play a role in the estradiol-modulated release of these hormones. Although the roles of ERα and the Gαq-coupled membrane estrogen receptor in the estradiol-induced desensitization response have not been directly tested, the selective

GPER1 agonist G-1 is sufficient to produce the desensitization of 5-HT_{1A}R signaling and knocking down GPER1 prevents estradiol-induced desensitization [27; 28].

Nonetheless, the mechanisms by which GPER1 signaling alter 5-HT_{1A}R signaling components to produce desensitization are still unclear. The release of OT and ACTH via 5-HT_{1A}R is dependent only on Gαz, not other members of the Gαi/o family [29]. However, Gαz protein levels in the membrane fraction [30] and total tissue homogenates of the PVN [28] are not altered by estradiol treatment. Gαz is active in the GTP-bound form and has a very slow intrinsic rate of GTP hydrolysis. RGSz1, a regulator of G protein signaling (RGS) protein, has a high affinity for Gαz and increases the rate of GTP hydrolysis by over 400-fold, effectively down-regulating Gαz downstream signaling [31; 32]. By this mechanism, increased RGSz1 could cause desensitization of 5-HT_{1A}R signaling. Indeed, our previous studies have shown that RGSz1 is up-regulated by estradiol and could thereby play an important role in the desensitization of 5-HT_{1A}R signaling [28; 33]. Two-day estradiol treatment increases RGSz1 mRNA, and several RGSz1 protein isoforms in the PVN, including a 29kd protein measured in the membrane fraction [33] and 45 and 55kd proteins measured in total homogenates of the PVN [28].

RGSz1 in the rat has a predicted molecular weight of 27kD based on its amino acid sequence [34]; however, multiple isoforms exist in the brain. RGSz1 has been shown to undergo posttranslational modification in isolated mouse synaptosomal membranes, including glycosylation, SUMOylation, and phosphorylation [35; 36], which may affect its subcellular localization and ability to regulate Gαz and thus contribute to desensitization of 5-HT_{1A}R signaling. This study is a comprehensive investigation of the effects of ER stimulation on post-translational modifications to RGSz1 protein isoforms. We focus on the subcellular localization of the various isoforms, especially the detergent-resistant microdomains (DRM) of the plasma membrane, where active Gαz and 5-HT_{1A}R are localized, to elucidate the ability of the protein to interact with Gαz and thereby attenuate 5-HT_{1A}R signaling.

Methods

Animals

Female ovariectomized (OVX) Sprague-Dawley rats (225–250g) purchased from Harlan (Haslett, MI) were housed two per cage in a temperature-, humidity-, and light-controlled room (12 h light/dark cycle). Food and water were available ad libitum. All procedures were conducted in accordance with the National Institutes of Health Guide for the Care and Use of Laboratory Animals and as approved by the University of Kansas Institutional Animal Care and Use Committee. All efforts were made to minimize animal discomfort and to reduce the number of animals used.

Drugs

17β-Estradiol-3-benzoate (EB) (Sigma-Aldrich, St. Louis, MO) was dissolved in 100% ethanol to a concentration of 25μg/ml and diluted to the final concentration with sesame oil. EB solution and sesame oil were administered at 0.4ml/kg. G-1 (1-(4-(6-

Bromobenzo[1,3]dioxol-5-yl)-3a,4,5,9b-tetrahydro-3H-cyclopenta[c]quinolin-8-yl)-ethanone), EMD Chemicals, Newark, NJ) was dissolved in 100% DMSO to a concentration of 5mg/ml and 10mg/ml and administered at 0.5ml/kg. (+)8-Hydroxy-2-dipropylaminotetralin ((+)8-OH-DPAT, Tocris, Ellisville, MO). (+)8-OH-DPAT was dissolved in 0.85% NaCl (saline) at a concentration of 0.2mg/ml and administered at a dose of 0.2mg/kg. Solutions were made fresh before injection.

Experimental Procedure

Animals were randomly grouped according to the following complete block design: vehicle/saline (n = 7), vehicle/DPAT (n = 8), EB/saline (n = 7), EB/DPAT (n = 8), G-1(2.5 mg/kg)/saline (n = 7), G-1(2.5 mg/kg)/DPAT (n = 8), G-1(5 mg/kg)/saline (n = 7), G-1(5 mg/kg)/DPAT (n = 8). Five days after OVX, rats were treated s.c. with EB (10μg/kg/day), G-1 (2.5 or 5 mg/kg/day), or vehicle (DMSO) once a day for 2 days. Eighteen hours after the last treatment, rats were injected with (+)8-OH-DPAT (0.2mg/kg, s.c) or saline and sacrificed via decapitation 15 minutes later. The EB dosing regimen was based on our previous time course and dose-response studies demonstrating that 10ug/kg/day of EB for two days produces the maximal desensitization of 5-HT_{1A}R signaling [28; 30]. At the time of experimental design, very little had been published regarding the systemic delivery of G-1 in rats; therefore, G-1 dose was calculated based on literature using implanted G-1 pellets in mice [37] and is similar to that used by Kastenberger et al., [38]. The 15 minute time period for sampling serum after 8-OH-DPAT was also based on a previous time course experiment which demonstrated that 15 minutes is the maximal response time for the effects of estradiol on ACTH and oxytocin [39]. Brains were removed and snap-frozen in dry-ice-cooled isopentane and then on dry ice. Trunk blood was collected in tubes containing 0.5ml 3M EDTA (pH 7.4). Brains and plasma were stored at −80°C until use.

Immunoblot assays

PVN was punched out from 300 μm-thick sections and tissue was homogenized as described previously [28]. Subcellular fractionation and isolation of the DRM from cortical tissue was performed as described previously [18]. Protein (10μg/lane) was resolved on a 12% SDS-PAGE gel followed by transfer to polyvinylidene fluoride (PVDF) membrane. The membranes were incubated in blocking buffer and probed overnight using the following primary antibodies: goat anti-SUMO2/3 1:200 (#sc-5231, Santa Cruz Biotechnology, Dallas, TX), mouse anti-phospho(Ser/Thr/Tyr) 1:100 (#E3074, Spring Biosciences, Pleasanton, CA), mouse anti-flotillin-1 1:2000 (#610820, BD Biosciences, San Jose, CA), mouse anti-Na+/K+ATPase α1 1:2000 (#sc-21712, Santa Cruz Biotechnology), rabbit anti-calreticulin 1:2000 (#Ab4, Abcam, Cambridge, MA), goat anti-EEA1 (C-15) 1:1000 (#sc-6414, Santa Cruz Biotechnology), mouse anti-βactin (C4) 1:20,000 (#69100, MP Biomedicals, Solon, OH). Samples to be probed with the RGSz1 antibody were prepared without β-mercaptoethanol to reduce background. RGSz1 antiserum was raised in rabbits against the last 15 amino acids of the C-terminal of RGSz1 by Biosynthesis (Lewisville, Texas). This RGSz1 antibody was previously shown to recognize a 27kD protein band in HEK293 cells transformed to over-express RGSz1but not in mock transformed cells [28]. Furthermore, the affinity purified RGSz1 antibody detected multiple protein bands at approximately the same molecular mass as in the current study, namely 27kD, 80kD, 90kD, 135kD and 145kD using

from 1.0 to 37 ng/lane of purified RGSz1 protein on a western blot. Detection of each of these bands was blocked by preadsorption of the RGSz1 antibody with purified RGSz1 protein [33]. In the current study the RGSz1 antibody was affinity purified and used at a dilution of 1:100. After washing, membranes were incubated with the appropriate secondary antibody conjugated with horseradish peroxidase at a dilution of 1:10,000. Bands were detected with ECL substrate solution (GE Healthcare Biosciences, Piscataway, NJ) using BioRad ChemiDoc XRS+ molecular imager (BioRad, Hercules, CA). Bands were analyzed densitometrically using ImageLab software (BioRad, Hercules, CA). Each band was normalized to actin and calculated as percent of the control group within each blot. All samples were run in triplicate and the average for each was used for the final quantification.

Glycoprotein isolation

Glycoproteins from the membrane fraction of rat cortex were isolated via binding to a column containing WGA resin using a Pierce glycoprotein isolation kit (Thermo Scientific Inc). Glycoproteins were eluted from the column using the provided elution buffer or by heating at 95°C in 200μl SDS-PAGE sample buffer for 5 minutes. Glycoproteins were examined on immunoblots probed with affinity-purified anti-RGSz1 (1:100).

Immunoprecipitation

Membrane and cytosol fractions of the cortex containing 500–1000 μg of protein were pre-cleared with 25 μl pre-washed protein G agarose beads (Invitrogen Carlsbad, CA) in total volume of 500 μl of IP buffer (50 mM Tris, pH 7.4, 10 mM EGTA, 100 mM NaCl, 0.5% Triton X-100, 20 mM NEM 1:100 protease inhibitor cocktail and 1:100 phosphatase inhibitor cocktail I and III) with rotation at 4°C for 1h. After centrifugation at 3000× g at 4°C for 5 min, the supernatant was incubated with primary antibody (4μg mouse anti-SUMO-1 (D-11), #sc-5308, Santa Cruz Biotechnology; 1:50 rabbit anti-RGSz1 or 4μg IgG control) and rotated at 4°C overnight. Pre-washed protein G beads (50 – 100 μl) were added to each tube and rotated at 4°C for 2 h. Protein G beads were pelleted by centrifugation at 1000× g, at 4°C for 3 min and then resuspended in 0.5 ml ice cold IP buffer. After washing, the protein complexes were eluted in 25 μl 2X sample buffer without β-mercaptoethanol by heating at 95°C for 5 min, then centrifuging at 3000×g for 5 min. The supernatant was collected and stored at −80°C until used for immunoblotting.

Radioimmunoassay of plasma oxytocin and ACTH

Plasma oxytocin and ACTH were determined by radioimmunoassay as previously described with minor modifications [17]. Radioactive ^{125}I oxytocin and ^{125}I ACTH (specific activity of each: 2200 Ci/mmol) were obtained from Perkin Elmer (Waltham, MA) and DiaSorin (Stillwater, MN), respectively. Intra-assay coefficients of variation were 3.93 for the oxytocin assay and 2.17 for the ACTH assay.

Statistical analysis

All experiments were performed in triplicate and data are expressed as means ± SEM. One- or two-way analysis of variance (ANOVA) and Student-Newman-Keuls post hoc tests were

conducted using a statistical program (Statview version 5.0 software, SAS Institute Inc., Cary, NC).

Results

RGSz1 isoforms have selective subcellular localization

The predicted molecular weight of RGSz1 is 27 kD; however, previous studies from our laboratory and others have demonstrated multiple RGSz1 bands on western blots [28; 33; 35; 36]. Western blotting with an affinity-purified RGSz1 antibody reveals a series of bands with differential distribution in the cytosol and membrane fractions in the cortex, hippocampus, hypothalamus and midbrain. Similar patterns of RGSz1 bands were seen in these brain regions but the relative abundance of individual RGSz1 isoforms varied.

To understand the functional importance of the different RGSz1 isoforms, we examined their subcellular localization via gradient centrifugation to separate the subcellular organelles based on their density (Figure 2A). The 135kD isoform colocalized with Na+/K +ATPase, a plasma membrane marker. Interestingly, while the 90kD and 50kD bands did not completely co-localize with any marker tested in the present study, they did localize with each other and showed some overlap with the plasma membrane marker (Figure 2B). The 80kD and 35kD bands were located in the early endosome, as marked by EEA1 (Figure 2C); however, as the fractions containing the early endosome also contain cytosolic markers [18], these isoforms could be located in the cytosol as well. Finally, the 45kD and 40kD bands were predominantly located in the ER, as determined by colocalization with calreticulin (Figure 2D).

Because activated Gαz proteins are localized in DRM of the plasma membrane [18], the RGSz1 isoform that facilitates GTP-Gαz hydrolysis would need to be located in the DRM. To this end, we isolated DRM with Triton X-100 treatment followed by sucrose gradient centrifugation. DRM fractions were identified by flotillin 1 (Figure 3A). Interestingly, the 135kD (Figure 3B) and 90kD (Figure 3C) proteins both distributed in two distinct populations: one was located in the DRM as marked by flotillin 1, and another one was located outside the DRM. The 50kD RGSz1 isoform localized entirely in the DRM (Figure 3C), while the 80kD band and the vast majority of the 40/45kD (unresolved) bands were not colocalized with the DRM, consistent with their location outside the plasma membrane (Figure 2).

Post-translational modification of RGSz1

To determine whether the increased molecular weights of the different RGSz1 isoforms could be due to post-translational modifications, we first used computer-assisted analysis of the RGSz1 amino acid sequence to predict potential modification sites. We found two possible sites for N-linked glycosylation (Center for Biological Sequence Analysis, http://www.cbs.dtu.dk/services/NetOGlyc/), as well as potential phosphorylation sites on several serine, threonine, and tyrosine residues (Center for Biological Sequence Analysis, http://www.cbs.dtu.dk/services/NetPhos/). In addition, we identified one SUMO consensus site via SUMOsp2.0 GPS program (http://sumosp.biocuckoo.org) (Figure 4A).

To examine glycosylation of RGSz1, glycoproteins from the membrane fraction of the cortex were isolated via binding to a column containing WGA resin, then eluted from the column using elution buffer. This procedure identified the 135kD band as the major glycosylated isoform of RGSz1 (Figure 4B); however, the yield was very low. Boiling the sample in SDS-PAGE buffer increased the amount of glycoproteins released from the WGA resin, and allowed us to detect significant bands at 135kD, 80kD, and 40kD, as well as several others (Figure 4C), suggesting that there are three major glycosylated RGSz1 protein isoforms. The lower intensity bands are likely either glycosylation of less abundant isoforms or represent degradation products.

We identified SUMOylated RGSz1using immunoprecipitation (IP) with SUMO 1 antibody followed by immunoblotting with the RGSz1 antibody. In the cytosol fraction, three bands were detected at 90kD, 50kD, and 45kD. In the membrane fraction, a 135kD band was detected, as well as a major band at 90 and 40kD (Figure 4D).

Next, anti-RGSz1 antibody was used to IP RGSz1 proteins from cytosol and membrane fractions of rat cortical tissue. Immunoblotting with anti-SUMO2/3 revealed a ladder of bands, with the clearest being at 35kD and 45kD in the membrane fractions and possibly the 135kD RGSz1 isoform (Figure 4F). Immunoblotting with an antibody against serine/threonine/tyrosine phosphorylation detected a strong band at 35kD and a lighter band at 40kD in both the cytosol and membrane fractions after RGSz1 IP (Figure 4E).

GPER1 stimulation alters RGSz1 isoforms in the PVN

To test the hypothesis that alterations in RGSz1 expression and post-translational modification after GPER1 stimulation underlie estradiol-induced desensitization of 5-HT_{1A}R signaling, we first examined the effect of 5 mg/kg G-1 and EB treatment on the expression of the different RGSz1 isoforms in the PVN.

In the cytosol fraction of the PVN, both G-1 and EB treatment had dramatic effects on RGSz1 expression (Figure 5A and B). Both pretreatments increased expression of the 80kD ($F_{(2,15)} = 28$, $p < .0001$) and 50kD bands ($F_{(2,17)} = 5.3$, $p = .017$) and decreased expression of the 135kD ($F_{(2,20)} = 7.7$, $p = .0033$) and 40/45kD bands ($F_{(2,17)} = 20$, $p < .0001$), with no change in the 35kD ($F_{(2,17)} = 1.2$, $p = .29$) relative to control. G-1 pretreatment increased expression of the 90kD band relative to both vehicle and EB ($F_{(2,17)} = 12$, $p = .0006$). (+)8-OH-DPAT had no effect on any of the RGSz1 isoforms (Figure 5C). Because the unmodified 29kD RGSz1 band is in such low abundance relative to the other isoforms, it is not easily detected with the affinity-purified antibody and thus was not measured in these experiments.

Interestingly, a 145 kD band is present in the PVN membrane but not detected in the other brain regions examined including the whole hypothalamus (Figure 5D). In the membrane fraction of the PVN, the predominant bands were at 145kD and 40/45kD (Figure 5E). However, due to the abundance of the band running at approximately 40kD, this band could also include the 45kD isoform. G-1 treatment produced a robust increase in the 145kD band ($F_{(2,15)} = 4.4$, $p = .03$), while EB treatment had no effect relative to control (Figure 5F). The 135kD band in the PVN was expressed in low abundance compared to the cytosol and other

brain regions, but was still quantifiable. Interestingly, both EB and G-1 treatment increased the 135kD isoform ($F_{(2,14)}$ = 6.1, p = .01) and decreased the 80kD isoform ($F_{(2,16)}$ = 28, p <. 0001). These results correspond to the changes in the cytosol, in which EB and G-1 treatment had the opposite effect on the 135kD and 80kD isoforms. The abundance of the 40kD band was not affected by treatment with EB or G-1 ($F_{(2,14)}$ = .25, p = .79). As in the cytosol, (+)8-OH-DPAT challenge had no effect on any of the RGSz1 protein isoforms (Figure 5G).

Peripheral G-1 administration reduces the hormone response to 5-HT_{1A}R stimulation

Baseline levels of plasma OT were unchanged in the treatment groups compared to vehicle (Figure 6A). Activation of 5-HT_{1A}R by (+)8-OH-DPAT increased plasma OT levels in vehicle-treated rats. The OT response was significantly reduced in the EB-treated group. The high dose of G-1 (5 mg/kg) significantly reduced the OT response comparable to EB; the low dose of G-1 (2.5 mg/kg) also reduced the OT response, although the effect was not as robust (two-way ANOVA: main effect of (+)8-OH-DPAT: $F_{(1,37)}$ = 493.6, p <.0001; main effect of pretreatment: $F_{(3,37)}$ = 8.541, p = .0002; interaction between pretreatment and challenge: $F_{(3,37)}$ = 5.840, p = .0023).

ACTH baseline response was not affected by any pretreatment (Figure 6B). Stimulation of 5-HT_{1A}R by (+)8-OH-DPAT increased ACTH levels in vehicle-treated rats. The magnitude of the ACTH response to (+)8-OH-DPAT was significantly reduced in EB-treated rats. Both doses of G-1 reduced ACTH significantly compared to vehicle and EB (two-way ANOVA: main effect of (+)8-OH-DPAT: $F_{(1,44)}$ = 842.6, p <.0001; main effect of pretreatment: $F_{(3,44)}$ = 7.707, p = .0003; interaction between pretreatment and challenge: $F_{(3,44)}$ = 7.180, p = .0005). Together, these data demonstrate that peripheral injection of G-1 is sufficient to reduce the 5-HT_{1A}R-mediated release of ACTH and oxytocin, similar to EB.

Discussion

The purpose of the present study was to identify RGSz1 isoforms that are positioned to alter 5-HT_{1A}R/Gαz signaling and determine if estradiol and specifically signaling through GPER1 impacts these RGSz1 isoforms. Our data suggest that the G-1-induced increases in the 135kD and perhaps the 145kD RGSz1 protein isoforms are a possible mechanism contributing to the desensitization of 5-HT_{1A}R signaling. This hypothesis is based on the findings that the 135kD RGSz1 protein isoform is located in the DRM where it is positioned to attenuate 5-HT_{1A}R/Gαz signaling and that stimulation of GPER1 by both estradiol and G-1 increased the levels of the 135kD RGSz1 protein isoform in the PVN. Although we identified three RGSz1 protein bands in the DRM migrating at approximately 135kD, 90kD and 50kD on immunoblots only the 135kD isoform was altered with EB and GPER1 stimulation. Interestingly, we found that while EB and G-1 treatment produced comparable changes in most of the RGSz1 bands measured, only G-1 increased a 145kD band in the membrane, resulting in a dramatic increase relative to control and EB treatment. That this expression was so markedly affected by G-1 treatment and not EB suggests that this isoform could contribute to the apparent sensitivity of the ACTH response to G-1 over EB treatment. ACTH release is under the control of CRH, and while the mechanism by which Gαz

mediates CRH release is still unclear, it could be particularly susceptible to regulation by the 145kD RGSz1 isoform. The 145kD band appears to be specific to the membrane fraction of the PVN; it is not seen in the cortex, hippocampus, amygdala, or even the other regions of the hypothalamus. The PVN does not contain enough protein to perform immunoprecipitation of RGSz1, so characterization of this isoform is difficult; however, its localization to the membrane fraction suggests that it could be localized to the DRM.

It is clear from the present study that signaling through GPER1 produces dramatic changes in posttranslational modifications of RGSz1 in the PVN. Except for the expression of the 145kD RGSz1 isoform which was only detected in the PVN, the expression of the other RGSz1 isoforms is more similar among the brain regions examined, albeit with some isoforms being more highly expressed than others. However, changes in RGSz1 protein after EB or G-1 treatment are dramatically different depending on the brain region. Previous work in our laboratory found that EB treatment produced a decrease in the 40kD RGSz1 isoform in the hippocampus but no change in the amygdala. Furthermore, a decrease of the 40kD band was observed in the PVN after EB treatment but this band was increased in the rest of the hypothalamus [30]. In contrast to our findings in the PVN, the effects EB and G-1 on RGSz1 in the frontal cortex are subtle and largely non-significant (data not shown). These results suggest that regulation of RGSz1 posttranslational modification is under local control, most likely due to the relative levels of specific types of ER expressed in each region.

Investigation of RGSz1 posttranslational modifications identified SUMOylation, glycosylation, and phosphorylation of RGSz1 isoforms. The present study demonstrated that the 135kD, 90kD, and 50kD RGSz1 isoforms are SUMOylated with SUMO1 and are the only isoforms located in the DRM. Remarkably, our previous studies demonstrated that SUMOylation of both 5-HT_{1A}R in the DRM and the 35kD Gαz isoform located in the DRM [18; 40]. Furthermore, treatment with EB and G-1 resulted in an increase in the 135kD RGSz1 in the membrane, with a corresponding decrease in the non-SUMOylated 80kD isoform in the cytosol. SUMOylation affects a variety of cellular processes including subcellular localization and control of protein-protein interactions. Vertebrates express three SUMO isoforms SUMO1, SUMO2 and SUMO3; SUMO2 and 3 are nearly identical and are referred to in combination as SUMO2/3. SUMO2/3 contains a SUMO consensus sequence, and can form poly-SUMO chains via isopeptide linkages; SUMO1 does not contain a consensus site and SUMOylation of a poly-SUMO chain with SUMO1 can thus serve to terminate the chain [41; 42]. We observed a ladder pattern of SUMO2/3 immunoreactivity after RGSz1 IP, which suggests chains of SUMO2/3. Addition of a SUMO1 molecule as a cap to a poly-SUMO2/3 chain could account for the increase in apparent molecular weight from 80kD to 135kD; thus SUMOylation may be acting as a molecular switch to increase RGSz1 in the DRM of the plasma membrane to regulate Gαz signaling. Since the DRM is the location of active GPCR signaling proteins, the increase in RGSz1 in the DRM would reduce the activity of Gαz signaling by hydrolyzing the activated GTP-bound Gαz to inactive GDP-bound Gαz. Our previous studies demonstrated that the 35kD Gαz isoform located in the DRM is decreased by EB treatment [18], and that 5-HT_{1A}R is also localized to the DRM [40]. The EB and G-1 induced increase of DRM-localized RGSz1 together with the EB-induced decrease of DRM-localized Gαz would reduce 5-HT_{1A}R signaling. Further

studies will be required to verify this putative mechanism. However, taken together with our previous studies [18; 40], our results suggest that SUMOylation with SUMO1 regulates key components of 5-HT_{1A}R signaling pathway in the PVN which regulates hormone release, including 5-HT_{1A}R, Gαz and RGSz1.

We found that the 35kD, and possibly the 50kD, RGSz1 isoforms are phosphorylated. Phosphorylation is critical in the control of many cellular pathways, and may be a regulator of non-nuclear SUMOylation as well [42]. Depending on the substrate, the negative charge of a phosphate group can enhance or inhibit SUMOylation [43; 44]. There is a serine residue (S159) adjacent to the SUMO consensus site that, if phosphorylated, could facilitate SUMOylation.

Protein glycosylation plays an important role in protein structure, signal transduction, cell-cell interactions, and hormone action [45; 46; 47]. Addition and editing of carbohydrate units to proteins occurs in the endoplasmic reticulum and Golgi apparatus. Here, we found that a major glycosylated form of RGSz1, at 40kD, localized to the endoplasmic reticulum. The RGSz1 proteins of greater molecular weights than 40kD are also glycosylated, suggesting that the 40kD band, which is the most abundant of the RGSz1 isoforms, may serve as a pool from which, once glycosylated, other modifications such as SUMOylation can be added or removed, thus regulating RGSz1 localization and function [48].

Recent studies in the mouse have demonstrated a similar RGSz1 immunoblot profile in the mouse brain, including high molecular weight bands (130–150kD) that were glycosylated [35] and mid-range molecular weight bands that were SUMOylated and phosphorylated [36]. These results cannot be compared directly with this present study, as the studies were conducted in different species (there is 86% homology between mouse and rat RGSz1), different receptor signaling systems were examined, and the antibodies used to detect RGSz1 were raised differently. However, the results from the current study are consistent with those from the mouse studies demonstrating that post-translational modifications including SUMOylation, glycosylation and phosphorylation of RGSz1 result in numerous protein bands detectable on western blots.

The long-term goal of the present study is to identify novel targets to more rapidly produce desensitization of 5-HT_{1A}R signaling in the PVN to improve the therapeutic effects of SSRIs [9; 15]. Two days of EB treatment produces a partial desensitization of 5-HT_{1A}R signaling and synergizes with fluoxetine to produce a rapid and complete desensitization [18]. This effect is mediated by GPER1, as knockdown of GPER1 expression prevents EB-induced desensitization, and intra-PVN injection of G-1 produces a partial desensitization of 5-HT_{1A}R signaling in the PVN [27; 28]. In the present study, we demonstrated that systemic G-1 treatment produces similar effects: first, a dose-dependent effect on OT release, with the higher dose reducing OT release by the same magnitude as EB. Second, both doses of G-1 produced a similar reduction of plasma ACTH which was even more robust than EB treatment consistent with our previous intra- PVN results [27].

Increasing the dose of EB or extending the length of treatment does not further reduce the hormone response to (+)8-OH-DPAT [18; 30]. EB, as a physiologically active estrogen,

activates all ER with slightly higher selectivity for the nuclear ERs over GPER1 (K_i of EB for ERα, ERβ, and GPER1 is 0.30 nM, 0.38nM, and 5.7 nM, respectively) [49]. ERβ is abundantly expressed in OT- and subset of CRH-expressing neurons in the PVN, while ERα is abundant in GABAergic neurons of the peri-PVN region [19; 20; 21]; EB treatment therefore stimulates ER with potentially opposing effects that may diminish the GPER1 response. G-1, on the other hand, is highly selective for GPER1 over ERα and ERβ (*Ki* for G-1 at GPER1 is 11 nM, with no significant binding at ERα or ERβ at concentrations up to 1 μM) [49]. Additionally, there is a partial estrogen response element in the promoter region of the CRH gene, and estradiol treatment has been shown to increase CRH mRNA and protein expression, as well as AVP mRNA, likely through an ERβ-mediated mechanism [50]. Selective stimulation of GPER1 with G-1 avoids an ERβ-mediated EB-induced increase in CRH, thus blunting the ACTH response. The selectivity of G-1 for GPER1 over the nuclear ERs may also explain the differential changes in RGSz1 isoform between G-1 and EB treatment.

In conclusion, the present results demonstrate that RGSz1 isoforms with different post-translational modifications are differentially distributed in subcellular organelle. In particular, we identified a SUMOylated 135kD RGSz1 isoform in the DRM where it can physically interact with activated Gαz and shut off 5-HT_{1A}R downstream signaling, thus reducing HPA axis activity. Most importantly, EB and G-1 treatment alter the expression of RGSz1 protein isoforms in the PVN, which is consistent with the hypothesis that RGSz1 post-translational modifications, especially SUMOylation, have a significant functional impact on RGSz1 activity and regulation of Gαz signaling in the PVN. Further studies are needed to test this hypothesis and determine the mechanisms by which GPER1 signaling increases SUMOylation. In addition, the present results demonstrate for the first time that peripheral delivery of the selective GPER1 agonist G-1 produces desensitization of 5-HT_{1A}R signaling. Peripheral delivery is significant for potential translation to preclinical and clinical studies, as peripheral injections are more feasible than intra-PVN delivery. Moreover, G-1 produced a more robust response than EB and would be less likely to produce off-target effects based on receptor selectivity. Our results provide evidence that targeting GPER1 and RGSz1 may provide a selective mechanism for the acceleration of SSRI therapeutic effects.

Acknowledgements

Funding for this study was provided by NIMH RO1MH058448.

References

1. Bao AM, Meynen G, Swaab DF. The stress system in depression and neurodegeneration: focus on the human hypothalamus. Brain Res Rev. 2008; 57:531–553. [PubMed: 17524488]
2. Gillespie CF, Nemeroff CB. Hypercortisolemia and depression. Psychosom Med. 2005; 67(Suppl 1):S26–S28. [PubMed: 15953796]
3. Nemeroff CB, Vale WW. The neurobiology of depression: inroads to treatment and new drug discovery. J Clin Psychiatry. 2005; 66(Suppl 7):5–13. [PubMed: 16124836]
4. Dinan TG. Serotonin and the regulation of hypothalamic-pituitary-adrenal axis function. Life Sci. 1996; 58:1683–1694. [PubMed: 8637392]

5. Bellido I, Gomez-Luque A, Garcia-Carrera P, Rius F, de la Cuesta FS. Female rats show an increased sensibility to the forced swim test depressive-like stimulus in the hippocampus and frontal cortex 5-HT1A receptors. Neurosci Lett. 2003; 350:145–148. [PubMed: 14550915]

6. Li Y, Raaby KF, Sanchez C, Gulinello M. Serotonergic receptor mechanisms underlying antidepressant-like action in the progesterone withdrawal model of hormonally induced depression in rats. Behav Brain Res. 2013; 256:520–528. [PubMed: 24016840]

7. Jorgensen HS. Studies on the neuroendocrine role of serotonin. Dan Med Bull. 2007; 54:266–288. [PubMed: 18208678]

8. Osei-Owusu P, James A, Crane J, Scrogin KE. 5-Hydroxytryptamine 1A receptors in the paraventricular nucleus of the hypothalamus mediate oxytocin and adrenocorticotropin hormone release and some behavioral components of the serotonin syndrome. J Pharmacol Exp Ther. 2005; 313:1324–1330. [PubMed: 15743927]

9. Gomez-Gil E, Navines R, Martinez De Osaba MJ, Diaz-Ricart M, Escolar G, Salamero M, Martin-Santos R, Galan A, Gasto C. Hormonal responses to the 5-HT1A agonist buspirone in remitted endogenous depressive patients after long-term imipramine treatment. Psychoneuroendocrinology. 2010; 35:481–489. [PubMed: 19762159]

10. Navines R, Martin-Santos R, Gomez-Gil E, Martinez de Osaba MJ, Imaz ML, Gasto C. Effects of citalopram treatment on hypothermic and hormonal responses to the 5-HT1A receptor agonist buspirone in patients with major depression and therapeutic response. Psychoneuroendocrinology. 2007; 32:411–416. [PubMed: 17337123]

11. Nikisch G, Mathe AA, Czernik A, Thiele J, Bohner J, Eap CB, Agren H, Baumann P. Long-term citalopram administration reduces responsiveness of HPA axis in patients with major depression: relationship with S-citalopram concentrations in plasma and cerebrospinal fluid (CSF) and clinical response. Psychopharmacology (Berl). 2005; 181:751–760. [PubMed: 15988572]

12. Rush AJ, Fava M, Wisniewski SR, Lavori PW, Trivedi MH, Sackeim HA, Thase ME, Nierenberg AA, Quitkin FM, Kashner TM, Kupfer DJ, Rosenbaum JF, Alpert J, Stewart JW, McGrath PJ, Biggs MM, Shores-Wilson K, Lebowitz BD, Ritz L, Niederehe G. Sequenced treatment alternatives to relieve depression (STAR*D): rationale and design. Control Clin Trials. 2004; 25:119–142. [PubMed: 15061154]

13. Steiner M, Romano SJ, Babcock S, Dillon J, Shuler C, Berger C, Carter D, Reid R, Stewart D, Steinberg S, Judge R. The efficacy of fluoxetine in improving physical symptoms associated with premenstrual dysphoric disorder. BJOG. 2001; 108:462–468. [PubMed: 11368130]

14. Bosker FJ, Cremers TI, Jongsma ME, Westerink BH, Wikstrom HV, den Boer JA. Acute and chronic effects of citalopram on postsynaptic 5-hydroxytryptamine(1A) receptor-mediated feedback: a microdialysis study in the amygdala. J Neurochem. 2001; 76:1645–1653. [PubMed: 11259482]

15. Lerer B, Gelfin Y, Gorfine M, Allolio B, Lesch KP, Newman ME. 5-HT1A receptor function in normal subjects on clinical doses of fluoxetine: blunted temperature and hormone responses to ipsapirone challenge. Neuropsychopharmacology. 1999; 20:628–639. [PubMed: 10327431]

16. Sargent P, Williamson DJ, Pearson G, Odontiadis J, Cowen PJ. Effect of paroxetine and nefazodone on 5-HT1A receptor sensitivity. Psychopharmacology (Berl). 1997; 132:296–302. [PubMed: 9292630]

17. Li Q, Muma NA, Battaglia G, Van de Kar LD. A desensitization of hypothalamic 5-HT1A receptors by repeated injections of paroxetine: reduction in the levels of G(i) and G(o) proteins and neuroendocrine responses, but not in the density of 5-HT1A receptors. J Pharmacol Exp Ther. 1997; 282:1581–1590. [PubMed: 9316875]

18. Li Q, Sullivan NR, McAllister CE, Van de Kar LD, Muma NA. Estradiol accelerates the effects of fluoxetine on serotonin 1A receptor signaling. Psychoneuroendocrinology. 2013; 38:1145–1157. [PubMed: 23219224]

19. Shughrue PJ, Lane MV, Merchenthaler I. Comparative distribution of estrogen receptor-alpha and -beta mRNA in the rat central nervous system. J Comp Neurol. 1997; 388:507–525. [PubMed: 9388012]

20. Miller WJ, Suzuki S, Miller LK, Handa R, Uht RM. Estrogen receptor (ER)beta isoforms rather than ERalpha regulate corticotropin-releasing hormone promoter activity through an alternate pathway. J Neurosci. 2004; 24:10628–10635. [PubMed: 15564578]

21. Suzuki S, Handa RJ. Regulation of estrogen receptor-beta expression in the female rat hypothalamus: differential effects of dexamethasone and estradiol. Endocrinology. 2004; 145:3658–3670. [PubMed: 15087431]

22. Rossi DV, Dai Y, Thomas P, Carrasco GA, DonCarlos LL, Muma NA, Li Q. Estradiol-induced desensitization of 5-HT1A receptor signaling in the paraventricular nucleus of the hypothalamus is independent of estrogen receptor-beta. Psychoneuroendocrinology. 2010; 35:1023–1033. [PubMed: 20138435]

23. Bryant DN, Dorsa DM. Roles of estrogen receptors alpha and beta in sexually dimorphic neuroprotection against glutamate toxicity. Neuroscience. 2010; 170:1261–1269. [PubMed: 20732393]

24. Hazell GG, Yao ST, Roper JA, Prossnitz ER, O'Carroll AM, Lolait SJ. Localisation of GPR30, a novel G protein-coupled oestrogen receptor, suggests multiple functions in rodent brain and peripheral tissues. J Endocrinol. 2009; 202:223–236. [PubMed: 19420011]

25. Revankar CM, Cimino DF, Sklar LA, Arterburn JB, Prossnitz ER. A transmembrane intracellular estrogen receptor mediates rapid cell signaling. Science. 2005; 307:1625–1630. [PubMed: 15705806]

26. Wang H, Ward AR, Morris JF. Oestradiol acutely stimulates exocytosis of oxytocin and vasopressin from dendrites and somata of hypothalamic magnocellular neurons. Neuroscience. 1995; 68:1179–1188. [PubMed: 8544991]

27. Xu H, Qin S, Carrasco GA, Dai Y, Filardo EJ, Prossnitz ER, Battaglia G, Doncarlos LL, Muma NA. Extra-nuclear estrogen receptor GPR30 regulates serotonin function in rat hypothalamus. Neuroscience. 2009; 158:1599–1607. [PubMed: 19095043]

28. McAllister CE, Creech RD, Kimball PA, Muma NA, Li Q. GPR30 is necessary for estradiol-induced desensitization of 5-HT(1A) receptor signaling in the paraventricular nucleus of the rat hypothalamus. Psychoneuroendocrinology. 2012

29. Serres F, Li Q, Garcia F, Raap DK, Battaglia G, Muma NA, Van de Kar LD. Evidence that G(z)-proteins couple to hypothalamic 5-HT(1A) receptors in vivo. J Neurosci. 2000; 20:3095–3103. [PubMed: 10777773]

30. Creech RD, Li Q, Carrasco GA, Van de Kar LD, Muma NA. Estradiol induces partial desensitization of serotonin 1A receptor signaling in the paraventricular nucleus of the hypothalamus and alters expression and interaction of RGSZ1 and Galphaz. Neuropharmacology. 2012; 62:2040–2049. [PubMed: 22251927]

31. Glick JL, Meigs TE, Miron A, Casey PJ. RGSZ1, a Gz-selective regulator of G protein signaling whose action is sensitive to the phosphorylation state of Gzalpha. J Biol Chem. 1998; 273:26008–26013. [PubMed: 9748279]

32. Wang Y, Ho G, Zhang JJ, Nieuwenhuijsen B, Edris W, Chanda PK, Young KH. Regulator of G protein signaling Z1 (RGSZ1) interacts with Galpha i subunits and regulates Galpha i-mediated cell signaling. J Biol Chem. 2002; 277:48325–48332. [PubMed: 12379657]

33. Carrasco GA, Barker SA, Zhang Y, Damjanoska KJ, Sullivan NR, Garcia F, D'Souza DN, Muma NA, van De Kar LD. Estrogen treatment increases the levels of regulator of G protein signaling-Z1 in the hypothalamic paraventricular nucleus: possible role in desensitization of 5-hydroxytryptamine1A receptors. Neuroscience. 2004; 127:261–267. [PubMed: 15262317]

34. Ross EM, Wilkie TM. GTPase-activating proteins for heterotrimeric G proteins: regulators of G protein signaling (RGS) and RGS-like proteins. Annu Rev Biochem. 2000; 69:795–827. [PubMed: 10966476]

35. Garzon J, Rodriguez-Munoz M, Lopez-Fando A, Garcia-Espana A, Sanchez-Blazquez P. RGSZ1 and GAIP regulate mu- but not delta-opioid receptors in mouse CNS: role in tachyphylaxis and acute tolerance. Neuropsychopharmacology. 2004; 29:1091–1104. [PubMed: 14997173]

36. Rodriguez-Munoz M, Bermudez D, Sanchez-Blazquez P, Garzon J. Sumoylated RGS-Rz proteins act as scaffolds for Mu-opioid receptors and G-protein complexes in mouse brain. Neuropsychopharmacology. 2007; 32:842–850. [PubMed: 16900103]

37. Zhang B, Subramanian S, Dziennis S, Jia J, Uchida M, Akiyoshi K, Migliati E, Lewis AD, Vandenbark AA, Offner H, Hurn PD. Estradiol and G1 reduce infarct size and improve

immunosuppression after experimental stroke. J Immunol. 2010; 184:4087–4094. [PubMed: 20304826]

38. Kastenberger I, Lutsch C, Schwarzer C. Activation of the G-protein-coupled receptor GPR30 induces anxiogenic effects in mice, similar to oestradiol. Psychopharmacology (Berl). 2012; 221:527–535. [PubMed: 22143579]
39. D'Souza DN, Zhang Y, Damjanoska KJ, Carrasco GA, Sullivan NR, Garcia F, Battaglia G, Doncarlos LL, Muma NA, Van de Kar LD. Estrogen reduces serotonin-1A receptor-mediated oxytocin release and Galpha(i/o/z) proteins in the hypothalamus of ovariectomized rats. Neuroendocrinology. 2004; 80:31–41. [PubMed: 15385710]
40. Li Q, Muma NA. Estradiol potentiates 8-OH-DPAT-induced sumoylation of 5-HT1A receptor: Characterization and subcellular distribution of sumoylated 5-HT1A receptors. Psychoneuroendocrinology. 2013; 38:2542–2553. [PubMed: 23786880]
41. Hickey CM, Wilson NR, Hochstrasser M. Function and regulation of SUMO proteases. Nat Rev Mol Cell Biol. 2012; 13:755–766. [PubMed: 23175280]
42. Wilkinson KA, Konopacki F, Henley JM. Modification and movement: Phosphorylation and SUMOylation regulate endocytosis of GluK2-containing kainate receptors. Commun Integr Biol. 2012; 5:223–226. [PubMed: 22808340]
43. Gregoire S, Tremblay AM, Xiao L, Yang Q, Ma K, Nie J, Mao Z, Wu Z, Giguere V, Yang XJ. Control of MEF2 transcriptional activity by coordinated phosphorylation and sumoylation. J Biol Chem. 2006; 281:4423–4433. [PubMed: 16356933]
44. Hietakangas V, Ahlskog JK, Jakobsson AM, Hellesuo M, Sahlberg NM, Holmberg CI, Mikhailov A, Palvimo JJ, Pirkkala L, Sistonen L. Phosphorylation of serine 303 is a prerequisite for the stress-inducible SUMO modification of heat shock factor 1. Mol Cell Biol. 2003; 23:2953–2968. [PubMed: 12665592]
45. Bustamante JJ, Gonzalez L, Carroll CA, Weintraub ST, Aguilar RM, Munoz J, Martinez AO, Haro LS. O-Glycosylated 24 kDa human growth hormone has a mucin-like biantennary disialylated tetrasaccharide attached at Thr-60. Proteomics. 2009; 9:3474–3488. [PubMed: 19579232]
46. Fogel AI, Li Y, Giza J, Wang Q, Lam TT, Modis Y, Biederer T. N-glycosylation at the SynCAM (synaptic cell adhesion molecule) immunoglobulin interface modulates synaptic adhesion. J Biol Chem. 2010; 285:34864–34874. [PubMed: 20739279]
47. Shental-Bechor D, Levy Y. Folding of glycoproteins: toward understanding the biophysics of the glycosylation code. Curr Opin Struct Biol. 2009; 19:524–533. [PubMed: 19647993]
48. Ellgaard L, Helenius A. Quality control in the endoplasmic reticulum. Nat Rev Mol Cell Biol. 2003; 4:181–191. [PubMed: 12612637]
49. Bologa CG, Revankar CM, Young SM, Edwards BS, Arterburn JB, Kiselyov AS, Parker MA, Tkachenko SE, Savchuck NP, Sklar LA, Oprea TI, Prossnitz ER. Virtual and biomolecular screening converge on a selective agonist for GPR30. Nat Chem Biol. 2006; 2:207–212. [PubMed: 16520733]
50. Solomon MB, Herman JP. Sex differences in psychopathology: of gonads, adrenals and mental illness. Physiol Behav. 2009; 97:250–258. [PubMed: 19275906]

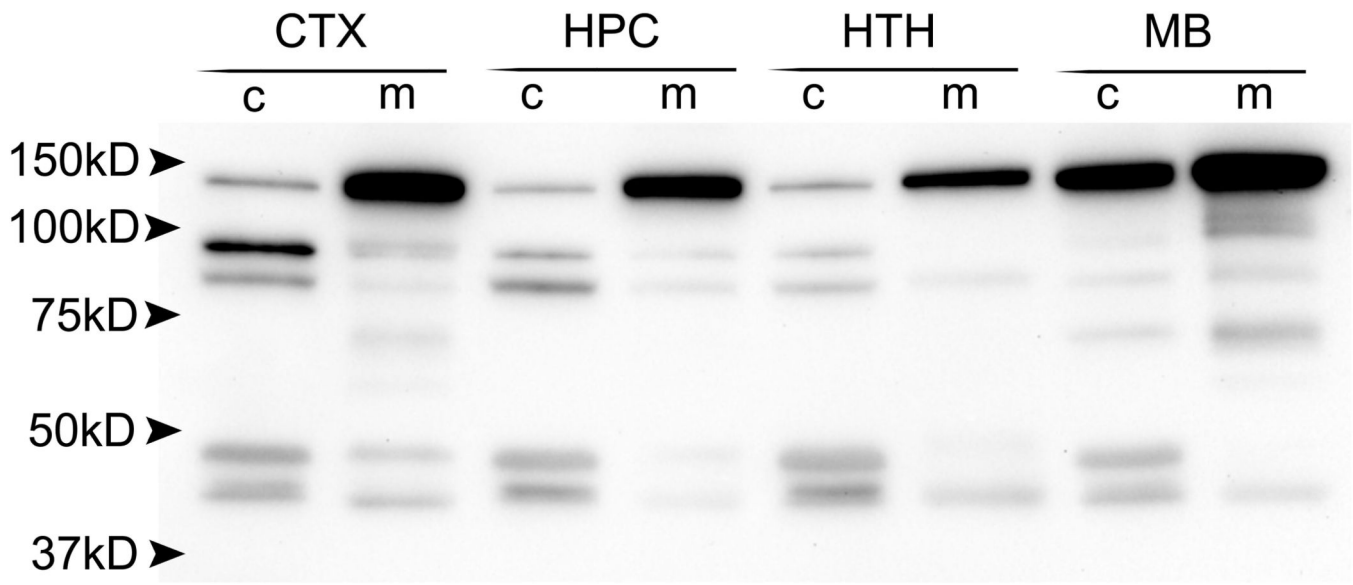

Figure 1.

RGSz1 protein in the rat brain. Immunoblot detection of RGSz1 expression in the cytosol (c) and membrane (m) fractions of the cortex (CTX), hippocampus (HPC), hypothalamus (HTH), and midbrain (MB) using affinity-purified anti-RGSz1 antibody.

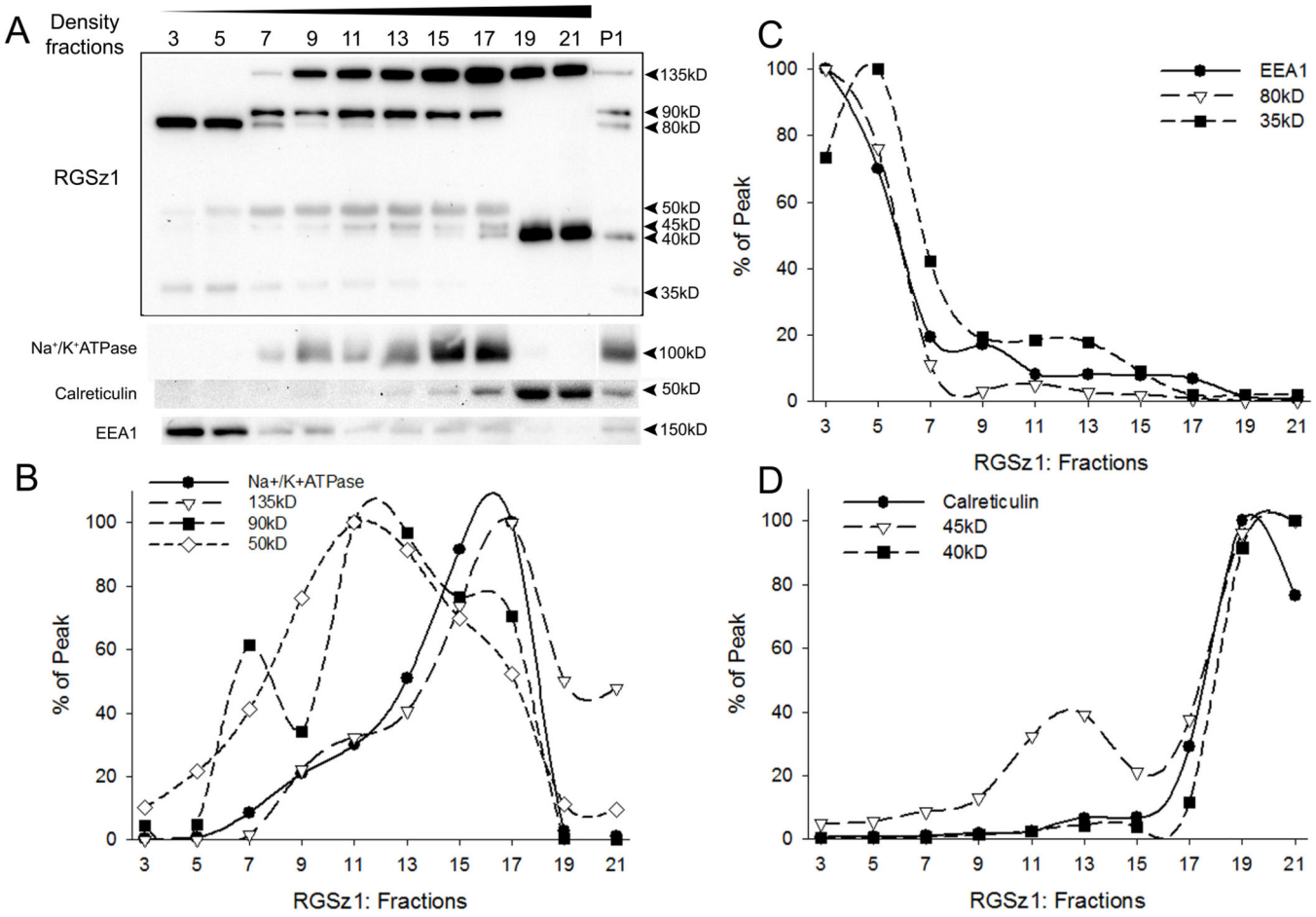

Figure 2.

Subcellular distribution of RGSz1 protein in subcellular fractions from discontinuous iodixanol gradient centrifugation prepared with rat cortex. Representative immunoblot is shown in (A). Graphical representations show the colocalization of RGSz1 with plasma membrane marker, Na+/K+ATPase (B); early endosome marker EEA1 (C); and ER marker calreticulin (D). Data are expressed as % of peak across fractions, and represent the average of three experiments.

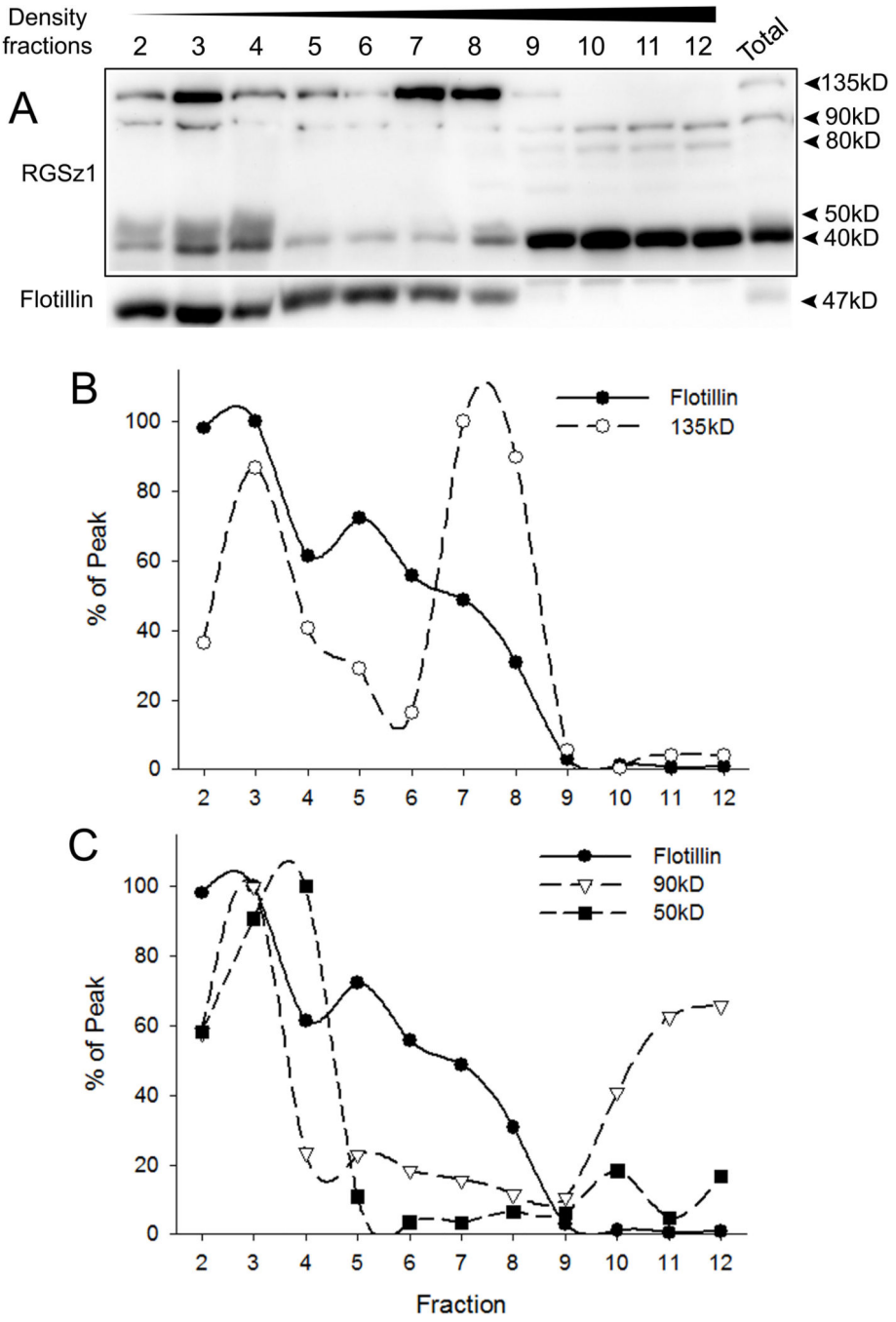

Figure 3.

Distribution of RGSz1 protein in sucrose gradient fractions of Triton X-100 treated cortex homogenates. (A) A representative immunoblot is shown. Fractions containing the DRM were identified by the DRM marker flotillin. Total: Triton X-100 treatment without sucrose gradient centrifugation. Graphical representations show the colocalization of RGSz1 with flotillin (B and C). Data are expressed as % of peak across fractions, and represent the average of three experiments.

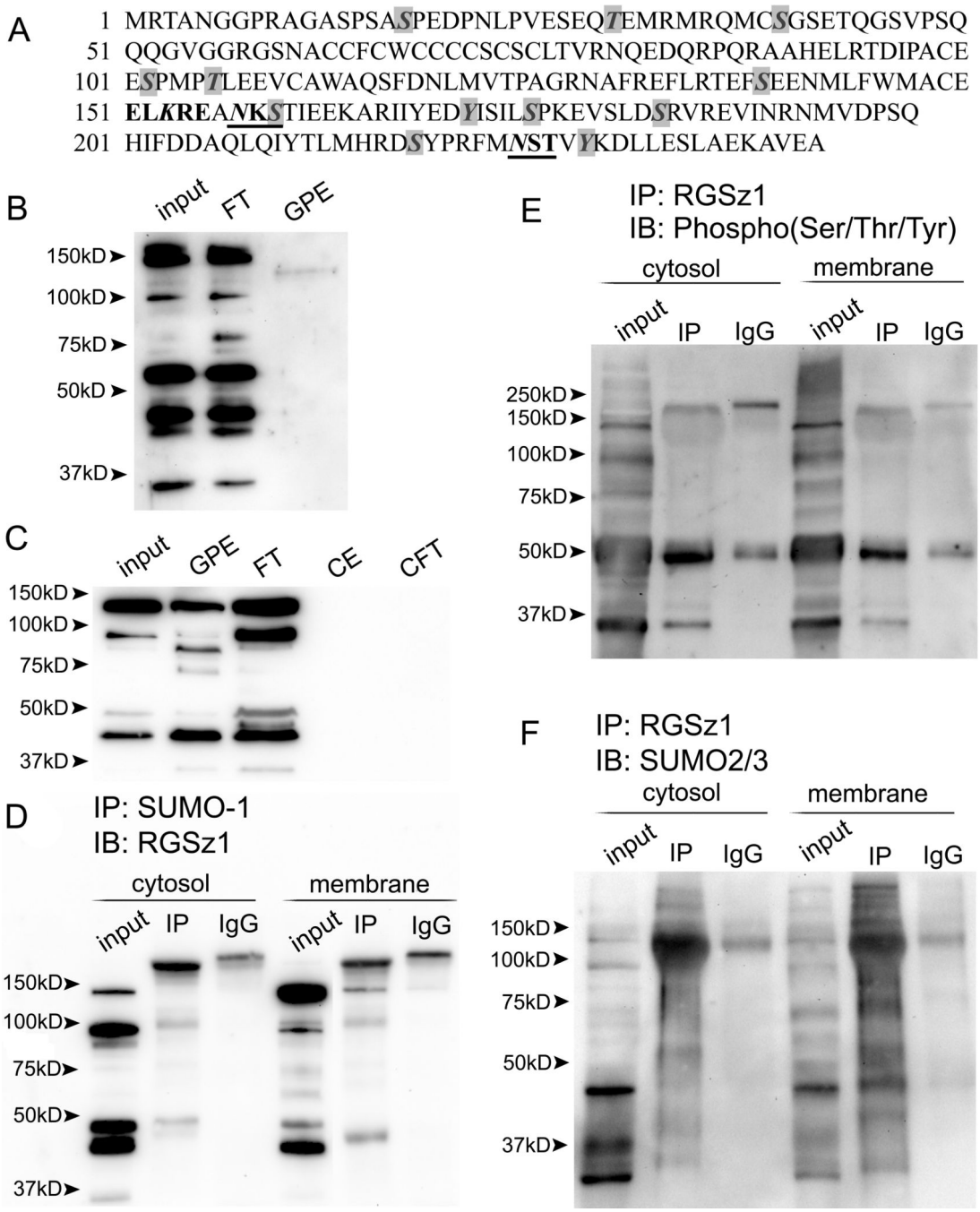

Figure 4.

Post-translational modifications of RGSz1. (A) Rat RGSz1 primary amino acid sequence. Predicted glycosylation sites are underlined and bolded; predicted SUMOylation site is bolded; predicted phosphorylation sites are shaded in gray. (B) RGSz1 immunoblot of glycoprotein isolated from cortical membrane fraction. Input: sample before isolation. FT: column flow-through. WGA: glycoproteins eluted from wheat germ agglutinin column. (C) RGSz1 immunoblot of isolated glycoprotein eluted from column by boiling in SDS-PAGE sample buffer. CE: control eluate (WGA column without protein added). CFT: control flow-

through. (D) Immunoprecipitation (IP) of SUMO-1 and immunoblot detection of RGSz1 in cytosol and membrane fractions of cortex. Input: sample before IP. IgG: mouse immunoglobin G control. IB: immunoblot. (E) IP of phosphorylated RGSz1 in cytosol and membrane fractions of cortex. IgG: rabbit immunoglobin G control. (F) IP of RGSz1 and immunoblot detection of SUMO2/3 in cytosol and membrane fractions of cortex. IgG: rabbit immunoglobin G control.

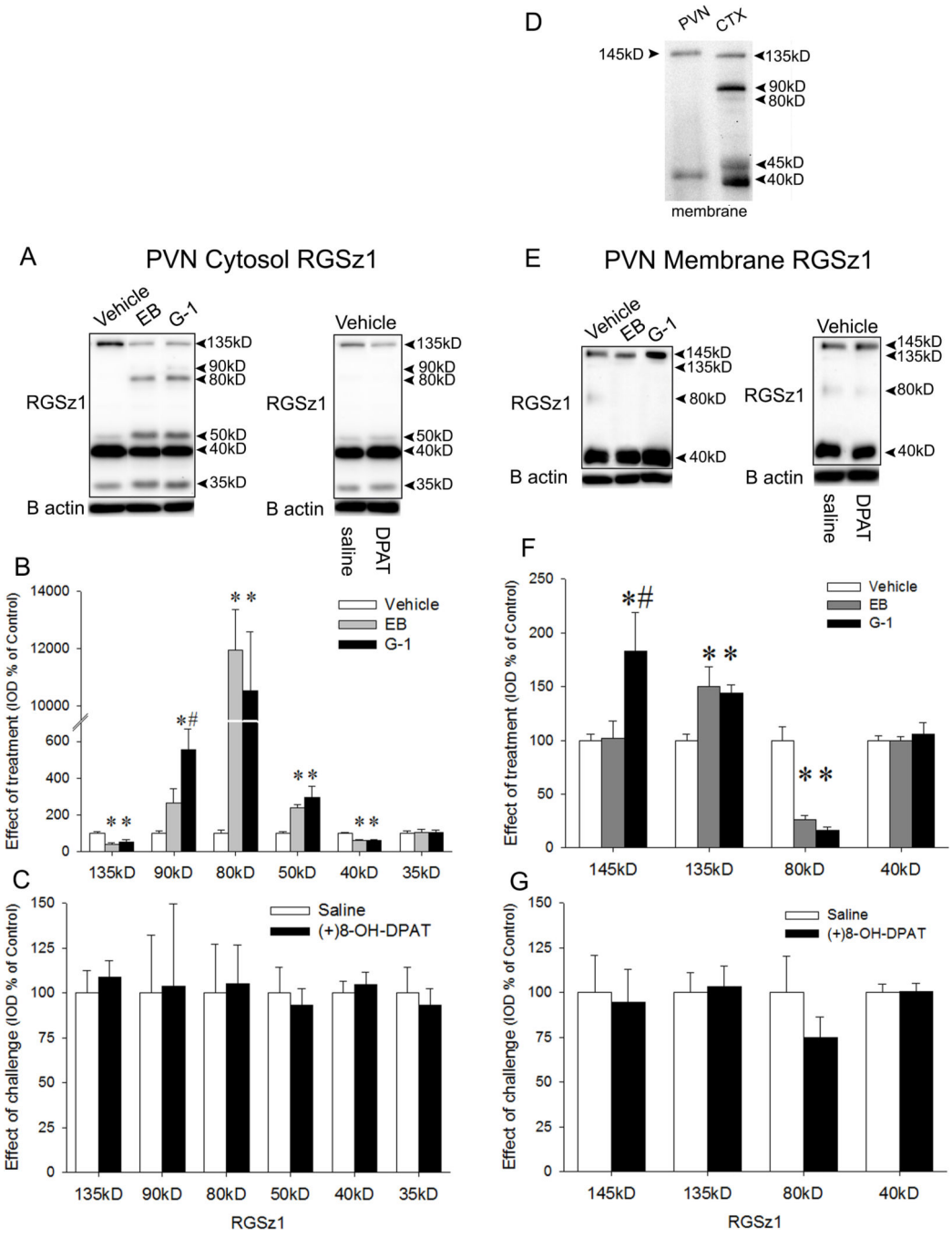

Figure 5.

(A) Representative immunoblot of cytosolic RGSz1 from the PVN of rats treated with 10μg/kg EB or 5mg/kg G-1 (left panel), or challenged with saline or (+)8-OH-DPAT (right panel), with β-actin as loading control. Effect of treatment (B) and challenge (C) is quantified and combined from three separate immunoblots. (D) Immunoblot comparison of RGSz1 high molecular weight bands in the membrane fractions of the PVN and CTX. (E) Representative immunoblot of RGSz1 from the membrane fraction of PVN of rats treated with 10 μk/kg EB or 5mg/kg G-1 (left panel), or challenged with saline or (+)8-OH-DPAT

(right panel), with β-actin as loading control. Effect of treatment (F) or (+)8-OH-DPAT challenge (G) is quantified and combined from three separate immunoblots. Bands were analyzed densitometrically (integrated optical density, IOD). Each band was normalized to β-actin and expressed as percent of control (vehicle or saline). Data are expressed as mean ± SEM (n = 4). Note that the 40 and 45kD RGSz1 bands did not appear to resolve into two separate bands as seen on the blots prepared with tissue from the subcellular fractionation preparations seen in Figure 2. The single band was quantified and labeled as a 40kD band although likely represents both the 40 and 45kD RGSz1 isoform. Probing for β actin was done on the same immunoblots as RGSz1 and matched to the correct lanes. (*) Significantly different from vehicle control; (#) significantly different from EB, $p < .05$ by Student-Newman-Keuls post hoc test.

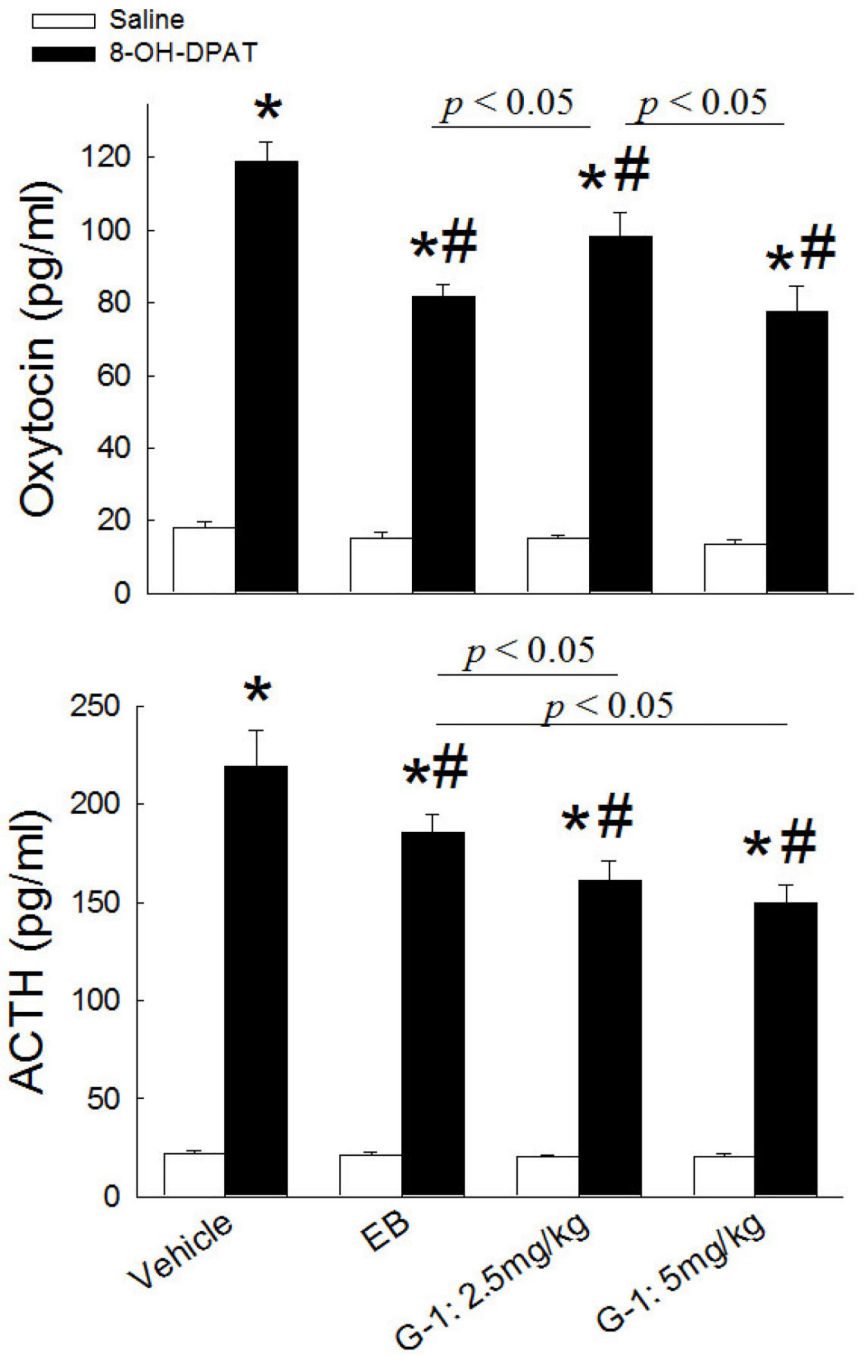

Figure 6.

Effects of 10μg/kg EB, 2.5mg/kg G-1, or 5mg/kg G-1 treatment for 2 days on plasma OT (A) and ACTH (B) levels in response to saline or (+)8-OH-DPAT challenge in OVX rats. The data are presented as the mean ± SEM (n = 7–8). (*)Significantly different from saline-challenged group with same treatment, p <.0001; (#)significantly different from (+)8-OH-DPAT-challenged vehicle group, p <.005 by Student-Newman-Keuls post hoc test.

Band	Subcellular Location	Modifications	Effect of EB Cytosol	Effect of EB Membrane	Effect of G-1 Cytosol	Effect of G-1 Membrane
145	Plasma membrane			X		↑
135	Plasma membrane	Glycosylation SUMO-1	↓	↑	↓	↑
90		SUMO-1	X		↑	
80	Endosome	Glycosylation	↑	↓	↑	↓
50		SUMO-1	↑		↑	
45	ER	SUMO-1 SUMO-2/3	↓	X	↓	X
40	ER	Glycosylation SUMO-1 Phosphorylation	↓	X	↓	X
35	Endosome	SUMO-2/3 Phosphorylation	X		X	

Figure 7.

Summary of RGSz1 isoform characterization. ↑: increased expression after treatment. ↓: decreased expression after treatment. X: no change in expression after treatment. Bands that were unmeasured in the PVN are left unmarked.